LIMITATION OF MOBILITY BY INTERCRYSTALLITE POTENTIAL BARRIERS WITH REGARD TO TUNNELING EFFECT

By D. Bednarczyk and J. Bednarczyk

Department of Solid State Physics, Pedagogical University, Częstochowa*

Effective mobility in a polycrystal has been calculated with due consideration paid to carrier tunneling through intercrystallite potential barriers. Numerical calculations were made and compared to experimental results for thin films of SnO_2. These films were used to show that the increase in mobility which accompanies an increase in impurities introduced into the film, as well as the small temperature dependence of mobility in strongly doped films can be explained by the influence of the tunneling effect.

1. Introduction

If, in a polycrystalline material, mobility changes exponentially with the inverse of temperature, the height of the barrier is generally estimated from the slope of the ln μ_{eff} $= f(1/T)$ curve. In many cases, the height of the barrier estimated in this way is too small to explain the large decrease in mobility. This has been observed in thin films of InSb [1], SnO_2 etc. At the same time, strongly doped, polycrystalline films show a large decrease in mobility and a small dependence on temperature. Furthermore, the effective mobility may increase with an increase in introduced impurities. These phenomena can be explained by the limitation placed on mobility by intercrystallite potential bariers, if we consider the tunneling effect in calculations.

2. Effective carrier mobility considering the tunneling effect

The limitation placed on mobility by intercrystallite potential barriers has already been discussed in many papers, e.g. [3–8]. Potential barriers decrease effective mobility, because not all carriers which come towards the barrier can cross over to the neighbouring

---

* Address: Zakład Fizyki Ciała Stałego, Wyższa Szkoła Pedagogiczna, Al. Zawadzkiego 13/15, 20-201 Częstochowa, Poland.

crystallite. It has been shown in Refs. [4, 8], that if the dimensions of the crystallites are several times larger that the mean free path, then the effective conductivity

$$\sigma_{\text{eff}} \simeq Nq\mu_0, \tag{1}$$

where N is the concentration of carriers crossing the potential barrier without reflection; q is the elementary charge, and μ_0 is the mobility of carriers in the material. N is, then, the concentration of carriers which carry a charge in an electric field from one crystallite to another. Because

$$\sigma_{\text{eff}} = n_k q \mu_{\text{eff}} \tag{2}$$

then

$$\mu_{\text{eff}} \simeq \mu_0 \frac{N}{n_k}, \tag{3}$$

where n_k is the carrier concentration in a crystallite. Formula (3) can be written as

$$\mu_{\text{eff}} \simeq \mu_0 \frac{\int\limits_0^\infty f_0(E, T) G(E) P(E) dE}{\int\limits_0^\infty f_0(E, T) G(E) dE}, \tag{4}$$

where $f_0(E, T)$ is the Fermi–Dirac distribution function, $G(E)$ is the density of states, and $P(E)$ is the probability that a carrier will cross of the potential barrier. If the concentration of impurities is so high that a donor (acceptor) band is formed, then $G(E)$ is combined density of states in the donor (acceptor) band and conduction (valence) band.

Let us consider carriers, which carry a charge in an electric field from one crystallite to another. That is carriers of energy higher than the barrier height which cross over the barrier, and carriers of energy lower than the barrier height which cross through the barrier as a result of the tunneling effect. In some cases the number of the latter carriers is comparable to, or even greater than the number of carriers which cross over the barrier. This occurs for films with a large concentration of free carriers, small effective mass and small crystallite dimensions. Then, the probability of crossing the potential barriers is relatively strong (even for small energies) so there is an evident influence of the tunneling effect on electrical properties.

To calculate the probability of crossing $P(E)$ in the energy function, the shape of the potential barrier should first be calculated from the Poisson equation. In a latter part of this paper an example of a numerical calculation of barrier shape, mobility and effective concentration for several temperatures, and donor concentrations will be given. The calculations have been made for an n-type semiconductor in which donor impurities are uniformly distributed in the volume of the crystallite, and the traps are placed on the surface of the crystallite.

3. Comparison of calculations with experimental results

Numerical calculations of concentration and mobility in thin SnO_2 films, obtained by means of cathode sputtering, [2] will be used as an example. Non-doped SnO_2 single-crystal in an n-type semiconductor becaused efects in this material give a shallow donor level. The activation energy of this level was estimated in Ref. [9] and is (0.024 ± 0.004) eV. Films of SnO_2 in Ref. [2] were self-doped (the concentration was marked $N_d^{(0)}$) and from the N_k antimony content in the cathode alloy 8 % was introduced into the film as donors. The donor concentration in the films was then

$$N_d = N_d^{(0)} + 0.08 N_k. \tag{5}$$

Influence of trap centres, which captured free carriers from the conduction band was observed in the temperature range in which the films were examined. The volume concentration of these traps was 3.2×10^{19} cm^{-3} larger than $N_d^{(0)}$ concentration. As the sizes of crystallites in films are small (diameter c. 100 Å), then, to calculate the barrier shape, a three-dimensional Poisson equation for a spherical crystallite was used [10]

$$\frac{d^2 \varphi(r)}{dr^2} + \frac{2}{r} \frac{d\varphi(r)}{dr} = - \frac{q^2}{\varepsilon \varepsilon_0} [n(r) + n_t(r) - p_d(r)], \tag{6}$$

where $n(r)$ is the concentration of free electrons in the conduction band, $n_t(r)$ is the electron concentration on the trap level, and $p_d(r)$ is the concentration of ionized donors. The position of the Fermi level has been determined from the condition of neutrality for a crystallite.

$$\int_0^R p_d(r) r^2 dr = \int_0^R [n(r) + n_t(r)] r^2 dr. \tag{7}$$

The solution of the Poisson equation, i. e. the barrier shape $\varphi(r)$ depends on: the radius of a crystallite R, temperature T, concentration of donors N_d and traps N_t, their distribution in a crystallite, position of the donor level E_d and trap level E_t and effective mass as well as on permittivity ε. In our calculations we assumed that donors are uniformy distributed in the sample, while traps are located on the surface of crystallites, as was suggested by the authors of Ref. [11]. Because of the large donor concentration, the overlapping of donor and conduction bands and peak of state densities on the donor level were considered in our calculations. The method of calculating the probability of electron transition through the potential barrier is given in Appendix A, while the method of calculating mobility in a SnO_2 single-crystal is presented in Appendix B. The concentration of carriers in a crystallite was calculated as a mean concentration of a crystallite's volume

$$n_{\text{eff}} = V^{-1} \int_V [n(r) + n_d(r)] dV \tag{8}$$

and effective mobility as:

$$\mu_{\text{eff}} = \mu_0 \frac{\int_V \int_E f_0(E, T) G(E) P(E) dE dV}{\int_V [n(r) + n_d(r)] dV}, \tag{9}$$

where $n_d(r)$ is the concentration of free electrons in the donor band. Evaluation of the mean value of both these values in the volume of the crystallite is necessary if we calculate the shape of the barriers from the three-dimensional Poisson equation, and it is not necessary for the one-dimensional case (large crystallites). In Eqs (8) and (9) we assume that the mobility of carriers in the conduction and donor bands is comparable.
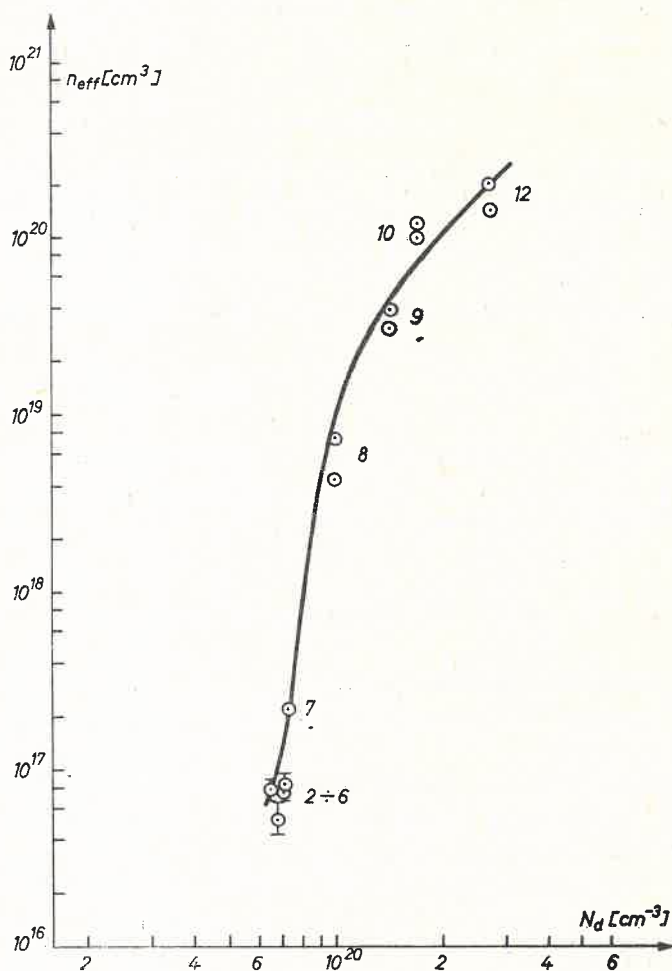

Fig. 1. Concentration of free carriers as a function of donor concentration. The solid line marks the results of calculations and points mark experimental results from Ref. [2] for thin SnO_2 films

The best agreement of numerical calculations with experimental results has been obtained for $N_d^{(0)} = 6.6 \times 10^{19}$ cm^{-3}, $E_t = 0.36$ eV and $R = 35$ Å. Because the surface concentration of traps for a spherical crystallite is $N_s = RN_t/3$, and $N_t = N_d^{(0)} + 3.2 \times 10^{19}$ cm^{-3}, then $N_s = 1.14 \times 10^{13}$ cm^{-2}. We assumed that $\varepsilon = 14$, $m_{eff}/m_e = 0.35$ and $E_d = 0.024$ eV.

Fig. 1 and Fig. 2 snow graphs of the effective concentration and mobility of carriers as a function of donor concentration. On Fig. 3 and Fig. 4 temperature dependences of those values for five different donor concentrations are presented. Results of numerical calculations for the parameter values mentioned above are marked with solid lines. Points
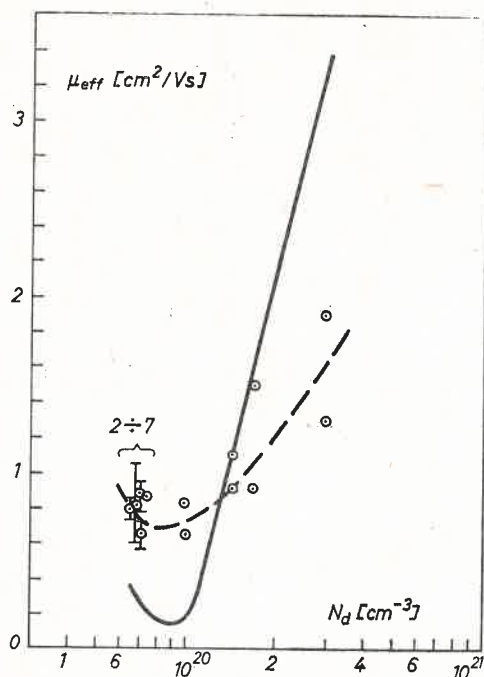

Fig. 2. Carrier mobility as a function of donor concentration. The solid line marks results of numerical calculations and points mark experimental results from Ref. [2]

were used to mark experimental results, obtained from examining the Hall effect for SnO_2 films [2]. Dependence of electrical conductivity as a function of N_k is shown on Fig. 5. The solid line shows the calculated conductivity, whereas points are used to mark experimental results obtained by various authors. The Hall mobility was measured only in some samples from Ref. [2] the conductivity of which has been marked in Fig. 5. Because of certain properties of the measuring apparatus [13], mobility was measured only in those samples in which conductivity was larger than 7×10^{-3} $(\Omega \, cm)^{-1}$.

In weakly doped films, where the volume trap concentration is larger than the donor concentration samples from cathodes 2 to 7 small values of mobility and concentration and strong temperature dependence of both these values has been observed. When donor concentration is greater than trap concentration the slope of the temperature curves decreases, while the value of mobility increases.

As in polycrystalline sample the sizes of crystallites are different, then formula (1) for conductivity is correct only when the shapes and heights of barriers do not depend on the dimensions of a crystallite. The barrier shapes for the most weakly and most strongly
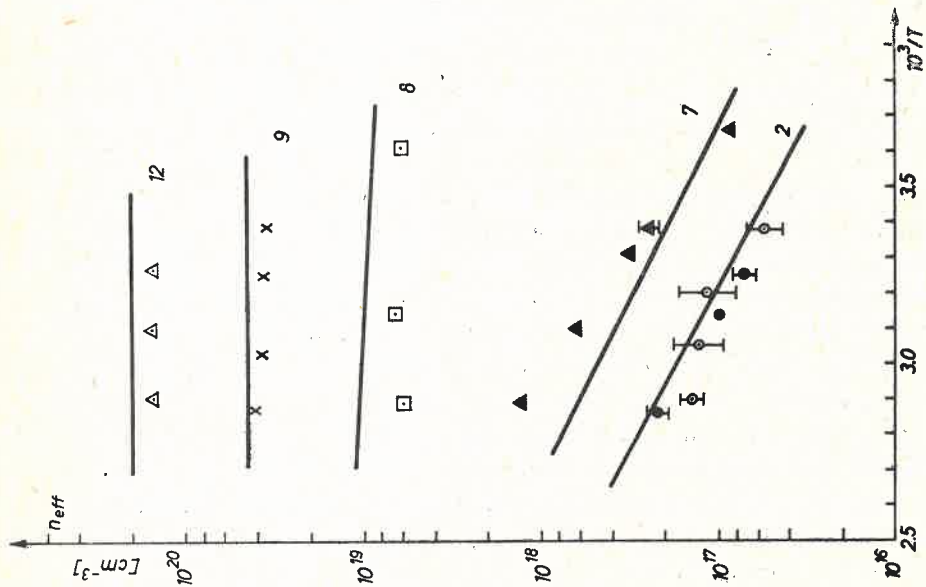
Fig. 3. Graphs ln $n_{eff} = f(1/T)$ for five donor concentrations. Solid lines mark the results of numerical calculations while points mark experimental results. The numbers denote cathodes from which samples were obtained
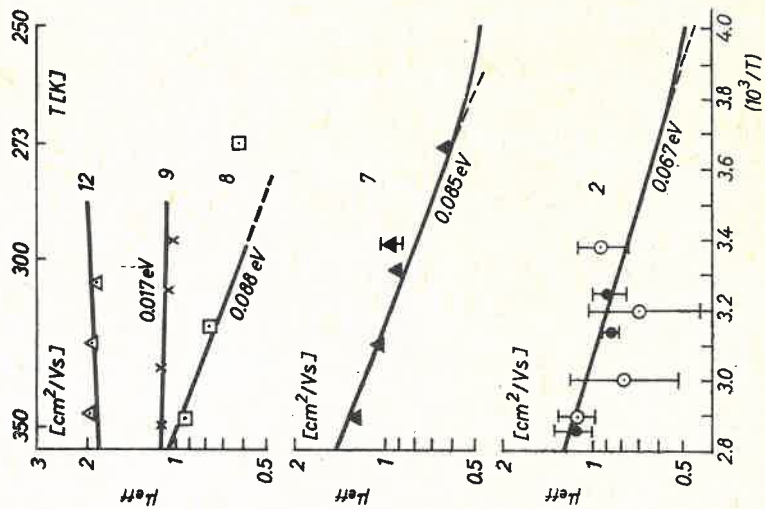
Fig. 4. Graphs ln $\mu_{eff} = f(1/T)$ for five donor concentrations. Solid lines mark slope of the curves obtained from numerical calculations for a given donor concentration. Points represent experimental results

doped films are shown in Fig. 6. In a weakly doped sample the bottom of the conduction band in small crystallites is strongly raised, while in a strongly doped sample the shapes of barriers in crystallites are similar. Electrical properties of a strongly doped sample only marginally depend on sizes of crystallites, whereas conductivity and effective mobility in weakly doped films depends mainly on properties of small crystallites acting as
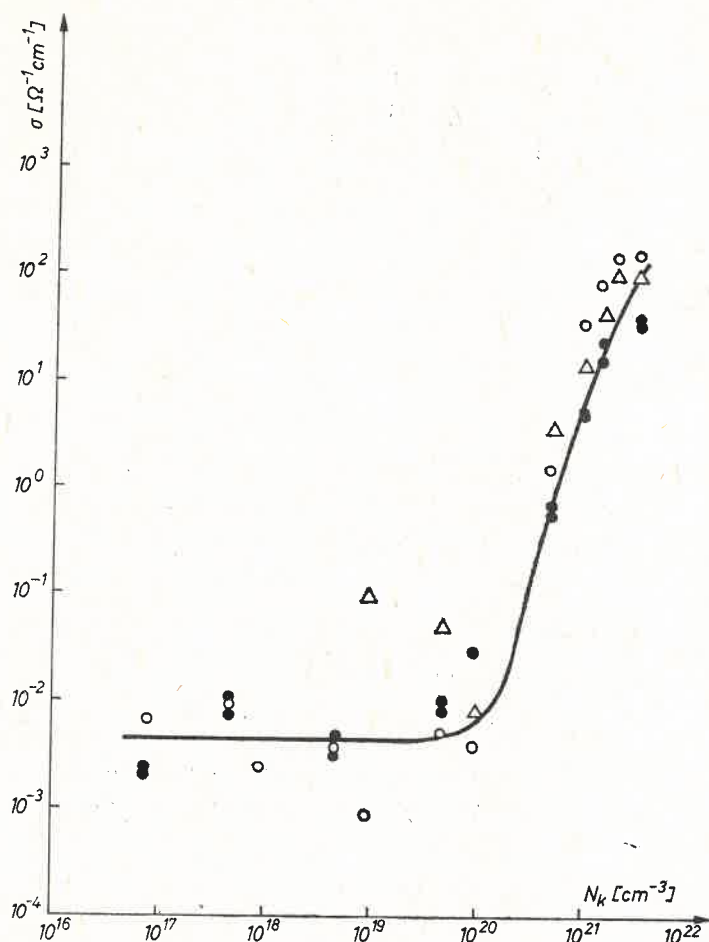

Fig. 5. Film conductivity as a function of content N_k in the cathode alloy. The solid line represents results of numerical calculations, points represents the experimental results for three series of samples: ● — from Ref. [2], ○ and △ — from Ref. [12]

"valves". The radius, for which the numerical calculations were made, is then smaller than that obtained in crystallographic examinaton [2].

Differences between the calculated value of mobility and the measured value originate from the fact that the distribution function of crystallites was not considered in the calculations. Furthermore, the Hall mobility was measured only in some samples. Especially, the

weakly doped samples of large resistivities (and probably of smaller mobility) were not measured.

In previous work concerning thin SnO_2 films [2] donor concentration $N_d^{(0)}$ was estimated and the value 8×10^{20} cm^{-3} was obtained which is different from the value 6.6×10^{19} cm^{-3} obtained now. It is because, previously, the irregular distribution of traps in the crystallite volume was not considered in the condition of neutrality. Regular trap
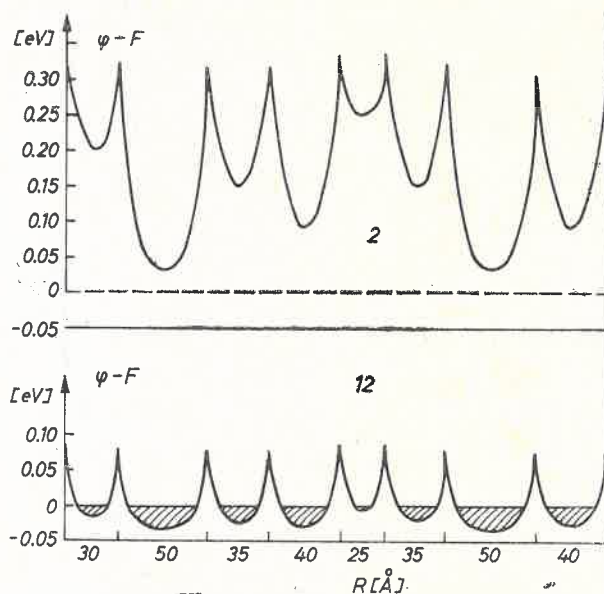

Fig. 6. An example of bending of the conduction band in strongly and weakly doped SnO_2 samples. Surface concentration of traps is the same for all crystallites i.e. $N_s = 1.14 \times 10^{13}$ cm^{-2}, donor concentration in sample 2 is $N_d = 6.6 \times 10^{19}$ cm^{-3} and in sample 12 is $N_d = 3 \times 10^{20}$ cm^{-3}

and donor distributions give $\varphi(r) \equiv 0$ which does not explain the small value of the mobility and its dependence on temperature. For small crystallites, mobility and concentration should be adjusted simultaneously considering the condition of neutrality in (7) with an irregular distribution of traps.

APPENDIX A

It will be assumed, like in Ref. [14], that donor states can be approximated by three-dimensional, rectangular potential wells. At the same time, it is known that shallow donor states in SnO_2 fulfil the assumptions of a hydrogen-like model [9], so the donor level is

placed in the middle of the potential well. The depth of the well is then $2\,|E_d|$ and the kinetic energy of the electron is $|E_d|$.

Potential wells will overlap if the parameter $\beta \leqslant 0$ (formula (3.6) from Ref. [14]). For SnO_2 this will occur when $N_d \gtrsim 2 \times 10^{18}$ cm^{-3}. Thus a donor band will be created for $N \gtrsim 2 \times 10^{18}$ cm^{-3} integrated with the conduction band. The critical value of N_d is in good
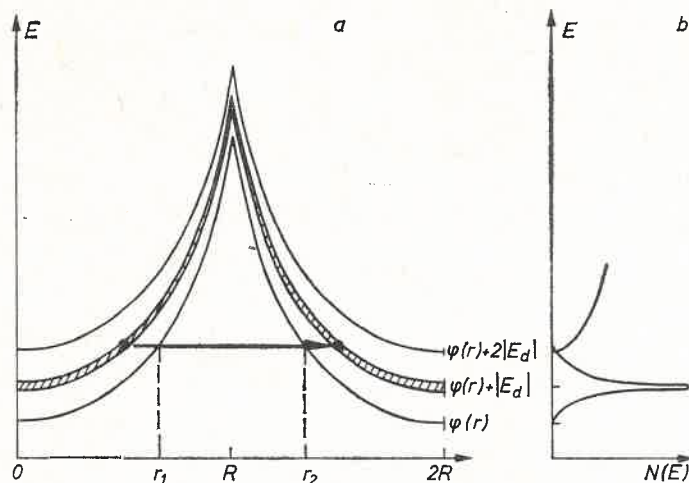

Fig. 7, a) Bending of energy bands near the crystallite surface. b) Density of states in the donor band and in the conduction band

agreement with experimental results for single-crystal SnO_2 [15]. When calculating the probability of carrier transition through the potential barrier it is convenient to utilise Fig. 7. Probability of electron transition was calculated from an approximated formula

$$P(E) \simeq \exp\left\{-2(2m_{\mathrm{eff}}/\hbar^2)^{1/2} \int_{r_1}^{r_2} [\varphi(r)-E]^{1/2}dr\right\}, \quad \text{if} \quad E < \varphi(R) \qquad \text{(A1)}$$

and

$$P(E) \equiv 1 \quad \text{if } E \geqslant \varphi(R).$$

As crystallite diameters are at least several times larger than the mean free path, the mean probability of a transition should be calculated in the mean solid angle 2π [16]. The probability is dependent on the normal component of momentum which is equivalent to

$$P(E, \alpha) = P(E\cos^2\alpha), \qquad \text{(A2)}$$

where α is the angle of incidence of electron in the barrier. The mean probability will then be

$$\langle P(E)\rangle = \frac{1}{2\pi} \int_0^{2\pi} P(E\cos^2\alpha)d\theta = \int_0^{\pi/2} P(E\cos^2\alpha)\sin\alpha d\alpha, \qquad \text{(A3)}$$

where the solid angle element $d\theta = 2\pi\sin\alpha d\alpha$. Mean value was calculated for $E < \varphi(R)$.

APPENDIX B

Dependence $N_d \gg N_c \simeq 6 \times 10^{18}$ cm^{-3} is valid for the SnO$_2$ samples discussed in this paper. That is why electron concentration in conduction band can be neglected for electron concentration in the donor band. As the density peak in the donor band will occur near E_d, it can be assumed that the energy of almost all electrons is $E = |E_d|$. Then Conwell--Weisskopf formula can be written (mean distance between donors is $l \simeq 1.27 \, N_d^{-1/3}$ [14])

$$\mu_I \simeq \frac{1.9 \times 10^{23}}{\ln\left[1 + 7.78 \times 10^{17}\left(\frac{E\varepsilon}{N_d^{1/3}}\right)^2\right]} \frac{E^{3/2}\varepsilon^2}{N_d\left(\frac{m_{\text{eff}}}{m_e}\right)^{1/2}}, \tag{B1}$$

where E is expressed in eV, and N_d in m^{-3}.

The scattering of phonons is considered as for non-doped crystals

$$\mu_P \simeq 200 \, \frac{\text{cm}^2}{\text{Vs}}\left(\frac{300 \text{ K}}{T}\right)^2, \tag{B2}$$
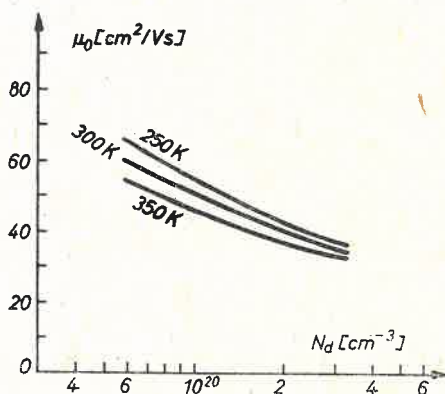

Fig. 8. Electron mobility in SnO$_2$ single-crystal as a function of impurity concentration for three temperatures

which is in accordance with the experimental results from Ref. [17]. Resultant mobility

$$\mu_0 = \frac{\mu_P \mu_I}{\mu_P + \mu_I}. \tag{B3}$$

Values of μ_0 for three temperature are shown on Fig. 8. As we consider the case of mono-energetic electrons, then the ratio of Hall mobility to drift mobility $\mu_H/\mu_d = 1$.

REFERENCES

[1] C. H. Ling, J. H. Fisher, J. C. Anderson, *Thin Solid Films* **14**, 267 (1972).
[2] D. Bednarczyk, J. Bednarczyk, *Acta Phys. Pol.* **A50**, 357 (1976); J. Bednarczyk, *Ph. D. Thesis*, Academy of Mining and Metallurgy, Cracow 1973 (in Polish).
[3] R. L. Petritz, *Phys. Rev.* **104**, 1508 (1956).
[4] J. Bednarczyk, D. Bednarczyk, *Acta Phys. Pol.* **36**, 1011 (1969).

[5] A. F. Mayadas, M. Shatzkes, J. F. Janek, *Appl. Phys. Lett.* **14**, 345 (1969).

[6] K. Lipskis, A. Sakalas, J. Viscas, *Phys. Status Solidi* (a) **5**, 793 (1971).

[7] J. C. Anderson, *Thin Solid Films* **18**, 239 (1973).

[8] D. Bednarczyk, J. Bednarczyk, *Acta Phys. Pol.* **A46**, 685 (1974).

[9] M. Nagasawa, S. Shionoya, *J. Phys. Soc. Jap.* **30**, 1213 (1971).

[10] D. Bednarczyk, J. Bednarczyk, A. Węgrzyn, 3rd International Conference on Thin Films, Budapest, August 1975; *Thin Solid Films* **36**, 165 (1976).

[11] Y. Mizokawa, S. Nakamura, *Jap. J. Appl. Phys.* **14**, 779 (1975).

[12] M. Jachimowski, E. Leja, J. Szczeklik, *Zeszyty Naukowe AGH* Nr 207, 71 (1969) (in Polish).

[13] D. Bednarczyk, J. Bednarczyk, A. Zamarski, *Acta Phys. Pol.* **A46**, 545 (1974).

[14] D. Bednarczyk, J. Bednarczyk, *Acta Phys. Pol.* **A46**, 315 (1974).

[15] J. A. Marley, R. C. Dockerty, *Phys. Rev.* **140A**, 304 (1965).

[16] D. Bednarczyk, *Ph. D. Thesis*, Academy of Mining and Metallurgy, Cracow 1973 (in Polish).

[17] M. Nagasawa, S. Shionoya, *Jap. J. Appl. Phys.* **10**, 472 (1971).